

MINISTRY OF EDUCATION AND TRAINING
**HO CHI MINH CITY UNIVERSITY OF TECHNOLOGY AND
EDUCATION**

TR. TRAN QUY HUU
ÀN QUY HỮU

**NON-ORTHOGONAL MULTIPLE ACCESS PROTOCOL FOR
ENERGY HARVESTING COOPERATIVE RELAYING RADIO
NETWORKS**

Specialization: Electronic Engineering
Specialized code: 62520203

SUMMARY OF THE DOCTORAL THESIS

HO CHI MINH CITY – 2023

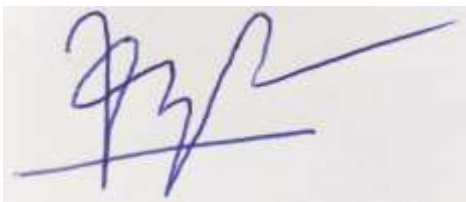
The work was completed at Ho Chi Minh City University of Technology and Education. Ho Chi Minh City

Supervisor 1: PGS. TS. Phan Văn Ca

A handwritten signature in blue ink, appearing to read 'phan van ca', with a long horizontal stroke extending to the right.

Phan Van Ca

Supervisor 2: TS. Viên Quốc Tuấn

A handwritten signature in blue ink, appearing to be a stylized 'VQT', with a long horizontal stroke extending to the right.

Vien Quoc Tuan

Reviewer 1:

Reviewer 2:

Reviewer 3:

The thesis will be defended in front of the Thesis Evaluation Council at the case level at Ho Chi Minh City University of Technology and Education on.....

ABSTRACT

This thesis has combined multiple access schemes, energy harvesting (EH), power splitting-based relaying (PSR), and time switching-based relaying (TSR) protocols, as well as the decode-and-forward (DF) protocol, in a simultaneous wireless information and power transfer non-orthogonal multiple access (SWIPT NOMA) system. This system can be applied widely to enable EH in cooperative relaying wireless networks, fifth-generation, and next-generation wireless communication systems.

Specifically, the thesis studies NOMA techniques, DF, and EH in SWIPT cooperative relaying systems. In the first network model, a half-duplex NOMA (HD NOMA) scheme is suggested for the SWIPT system to allocate power for two users, one of which is considered as a relay station that performs both EH and DF on the received signal. The suggested scheme makes use of a power splitting (PS) receiver architecture which enables both information processing and EH at the relay station. The performance of the suggested scheme is analyzed in terms of outage probability (OP), throughput and ergodic rate. Specifically, closed-form expressions are derived for the OP at both users, while the analytical results of the throughput and ergodic rate are obtained for DLT and DTT modes, respectively. It is shown that, with the NOMA adaptation, an improved outage performance is attained in terms of throughput and ergodic rate compared to the conventional orthogonal multiple access (OMA). The energy efficiency (EE) is also derived for the suggested HD NOMA systems. Our numerical results depict that the NOMA attains a better EE performance than the conventional OMA.

Second, PSR/TSR protocols are successively used for SWIPT in a NOMA based cooperative relaying wireless-powered networks (CRWPNs) containing a base station and two destination nodes among which one plays the role as a relay station to assist the communication between the base station and the far node. Additionally, DF is considered at the relay station over two transmission modes, i.e., Delay-limited Transmission (DLT) and Delay-tolerant Transmission (DTT). In performance analysis, closed-form expressions of OP, throughput, ergodic rate, and EE are derived for the PSR and TSR protocols with DLT and DTT

modes in the NOMA-based CRWPNs. Next, the performance is analyzed to realize the impacts of EH time, EH efficiency, PS ratio, source data rate, and the distance between the nodes. Furthermore, the impacts of these parameters on the OP and ergodic rate of two users at high SNR regime are also evaluated. The simulation results demonstrate that the performance for CRNOMA outperforms that for OMA. For performance comparison between two protocols, the TSR achieves higher throughput, ergodic rate, and EE than the PSR. The investigation and evaluation of performance metric versus different distances between from the base station to relay station and comparison between direct and indirect links with different path losses are also performed.

In the last model, closed-form expressions of the performance, i.e., OP, throughput, ergodic rate and EE, are derived for the PSR protocol with DLT and DTT modes, and direct link. This performance of the system model with direct link is compared to that for C-NOMA indirect link and OMA. The simulation results show that the C-NOMA with direct link achieves a better performance than that for the C-NOMA indirect link and OMA. The impacts of above-mentioned parameters on the direct link are evaluated via the numerical simulation results to realize the changes of the performance. These influences are the foundation for selecting parameters with appropriate values for the system model to strike a balance between performance and user device terms.

Chapter 1: OVERVIEW

1.1. The urgency of the subject

Mobile communication is one of the essential fields in human society. As society develops, people's needs for communication and online interaction are increasing. Along with this evolution, wireless networks using nG technologies, as well as the next generation networks, have emerged and will continue to emerge to serve people's needs. The explosion in the number of access devices, various types of networks, and services have led to limitations in access speed, capacity, bandwidth, energy, and signal transmission delay.

In telecommunications networks, these limitations become evident across networks ranging from 1G to 4G. Within these networks, the employed access technique is orthogonal multiple access (OMA), which encompasses methods like TDMA, CDMA, FDMA, and OFDM. This thesis concentrates on investigating the challenge of energy harvesting at relay stations, with the aim of extending the operational duration of relay stations in NOMA systems. The investigation involves cooperative relaying and simultaneous power transmission, utilizing the PSR, TSR, and DF protocols for energy harvesting. These protocols facilitate the tasks of harvesting energy, decoding information, and forwarding data from the source node to the destination node. NOMA has recently emerged as a highly promising technique for deployment in 5G and next-generation networks. It aims to overcome the challenges posed by current technologies, such as energy efficiency, latency, and fairness among user devices [80], [87]-[88]. One of the notable characteristics of the NOMA technique is its ability to enable multiple user devices to share the same time, frequency, and/or code domain resources [80]. In this approach, a robust user device located closer to the base station (NU) receives a lower power allocation factor compared to a weaker user device, situated farther away from the base station (FU) and characterized by inferior channel conditions. This allocation strategy ensures equitable treatment of user devices [4], [6], [87], [89]. The two primary techniques implemented within NOMA are superposition coding [88] and successive interference cancellation [87]-[88]. An extended version of NOMA known as Cooperative NOMA (C-NOMA) [91]-[92] leverages user equipment with stronger channel conditions, particularly devices in transit, to facilitate the

forwarding of information to other user devices characterized by weaker channel conditions. Consequently, C-NOMA contributes to expanding the coverage area of base stations and enhancing the overall performance of the NOMA system. In the current landscape, numerous research groups are actively investigating NOMA techniques for 5G and next-generation networks. Notably, the team at Middlesex University [1]-[2] is dedicated to addressing energy-related challenges within the system, encompassing NOMA systems in heterogeneous cloud radio access network (HCRAN) networks, as well as spectrum sensing problems in cognitive radio networks. Additionally, the research group at the University of Manchester [3] is focused on exploring collaborative NOMA and transition selection algorithms, integrating energy harvesting (EH) within the network through the application of NOMA technology. Energy harvesting from radio frequencies offers a solution to energy constraints and the extension of battery life in electronic devices, wireless sensors, and relay stations within wireless communication networks [91]-[92]. In the context of relay stations, energy harvesting is integrated into the initial phase of the transmission time block. The energy harvested serves two main purposes: i) powering the relay station itself, and ii) forwarding the decoded information to the destination node. The integration of SWIPT with C-NOMA in 5G systems has demonstrated enhanced EE and broader coverage compared to conventional OMA techniques [31], [89]. Moreover, a relay station employing SWIPT within the C-NOMA framework can not only enhance the originality and reliability of transmitted data for weak user devices by relaying information to remote user devices, but also contribute to the improvement of the overall system [93]. SWIPT-based relay stations utilize the PSR and TSR protocols to implement energy harvesting and information processing [4], [6], [29], [94]. In [95], the research delved into the total throughput of user devices within the SWIPT-based C-NOMA system. Both approximate and explicit mathematical expressions for the outage probability were derived. Additionally, [96] introduced two SWIPT-based protocols, namely CNOMA SWIPT-PS and CNOMA-SWIPT-TS. The efficacy of these proposed mechanisms was demonstrated to surpass that of conventional OMA methods and the approach presented in [97]. In [90], the study investigated SWIPT within the framework of the C-NOMA system. A unified design for Power Splitting (PS) and Time Switching (TS) factors was proposed to enhance system performance. The paper also furnished analytical expressions for the outage

probability concerning both near and distant user devices. Additionally, [98] examined PSR-based SWIPT for C-NOMA. Compared to the approach in [99], this protocol substantially reduces the outage probability for powerful user devices while boosting overall system throughput. The work in [100] showed that the outage probability and throughput of the proposed Time Switching Ratio (TSR) protocol outperforms those of the conventional TSR protocol. Within forwarding-enabled C-NOMA, two primary data forwarding mechanisms exist: Decode and Forward (DF) and Amplify and Forward (AF) [87]. In the context of C-NOMA-based forwarding, remote user devices often receive signals initially transmitted by the base station, which are then forwarded from relay stations [100]-[104]. This is due to various obstacles in the transmission path [4], [6], [105]. Nevertheless, within obstacle-free system models, these remote user devices can receive signals from both cooperative relay stations and the base station, thus involving a C-NOMA-based relay station with direct links [53], [106]-[108]. In [106], a dynamic DF mechanism based on C-NOMA for downlink transmission was introduced. The OP expression for this mechanism was derived using point process theory. Furthermore, [109] presented three cooperative relay mechanisms within a DF-based C-NOMA system. The performance of these proposed mechanisms surpasses that of DF cooperative forwarding without direct links and the approach of superimposing signal transmission to multiple user devices without forwarding. In [110], an investigation into a DF-based C-NOMA system featuring a direct link between the base station and weak user equipment was conducted. Additionally, [111] explored a device-to-device cooperation system using NOMA, wherein the base station communicates simultaneously with all user devices. The study proposed two decoding strategies: the single-signal decoding scheme and the maximum-ratio-combination (MRC) scheme decoding. Simulation results demonstrated that both the overall average speed and the outage probability (OP) are superior to those observed with conventional NOMA schemes. In [112], the authors introduced a protocol enabling dynamic switching between direct and indirect methods within a C-NOMA system involving two user devices. The analysis results have demonstrated the superiority of the proposed protocol compared to conventional C-NOMA protocols. Additionally, [77] presented the outage performance analysis of a dual DF-based SWIPT NOMA system featuring direct links. The use of relay stations to transmit information from a base station to a

destination node and simultaneously perform EH from RF sources has been extensively investigated within current technologies, including OFDMA and SWIPT/WPT [113] - [115]. In [113], a relaying selection scheme, namely OFDMA relaying selection, was proposed for OFDM multihop cooperative networks with L relays and M hops ($M, L \geq 2$). The end-to-end outage performance of the proposed approach was evaluated and compared to that of the OFDM relaying selection approach. In [38], a relaying selection scheme was investigated in a two-hop relay-assisted multi-user OFDMA network with K fixed relays and L users ($2 \leq L \leq K$), where the end-nodes exploited the SWIPT mechanism based on the PS technique. This relaying selection is to optimize the PS ratio of the end nodes as well as the relay, carrier, and power assignment so that the sum-rate of the system was maximized under the harvested energy and transmitted power constraints. In [115], a survey of the SWIPT and WPT assisted energy harvesting techniques was presented. The survey provided a detailed description of various potential emerging technologies for the fifth generation (5G) communications with SWIPT/WPT.

The contributions of this thesis are as follows:

Firstly, the cooperative relaying NOMA system leverages the application of PSR and TSR protocols within the SWIPT mechanism. Secondly, the study involves examining performance parameters such as OP, throughput, ergodic rate, and EE. This analysis aims to facilitate comparisons between the PSR and TSR protocols, as well as between NOMA and OMA. Thirdly, the research focuses on constructing explicit mathematical expressions to quantify system performance. This includes system OP, throughput, ergodic rate, and EE. These mathematical expressions encompass scenarios involving the PSR protocol with both DLT and DTT, cooperative relaying, and direct link. The performance of the direct-link system model was compared with that of C-NOMA using cooperative relaying, as well as the comparison between C-NOMA and OMA. Simulation results have demonstrated that C-NOMA with direct link achieves superior performance compared to forward C-NOMA, and C-NOMA outperforms OMA. Furthermore, the study examines the impact of parameters such as EH execution time, power division factor, EH performance efficiency, source data rate, and base station-to-relay distance. These factors are investigated to understand their influence on OP, throughput, ergodic rate, and EE, as well as their impact on the two PSR and TSR

protocols. The effects of these parameters on the direct link are evaluated against numerical simulation results to assess changes in system performance. These insights serve as a foundation for selecting appropriate parameter values in the system model, aiming to strike a balance between performance factors and among users.

Chapter 2: THEORETICAL BASIS

2.1. Non-orthogonal multiple access

2.1.1. Introduction

NOMA engineering has been developed to cater to the requirements of 5G and next-generation networks. Within this framework, two fundamental technologies in the power domain of NOMA engineering are stacked coding and serial noise suppression. These advancements play pivotal roles in enhancing the capabilities of the NOMA system. To enable base stations to effectively transmit information to users characterized by weak channel conditions, the concept of cooperative NOMA is harnessed in these network models. Within the realm of cooperative NOMA, users endowed with favorable channel conditions contribute to facilitating the transmission of information from the source to the intended recipient—users grappling with inferior channel conditions. In the context of collaborative NOMA, a central issue revolves around powering the relay users, ensuring their sustained operation. An approach to address this challenge involves harnessing the energy collected from the RF radio signals supplied by the transmitter. This harvested energy serves as a potential power source within a collaborative NOMA system.

2.1.2. Energy harvesting in NOMA downlink cooperation with SWIPT

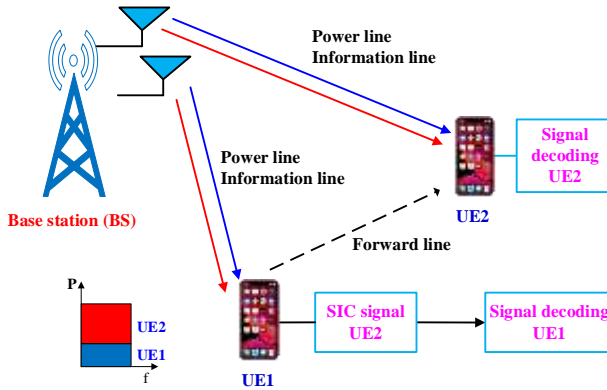


Figure 2.1: Simultaneously energy harvesting and information transmission model by applying cooperative NOMA based on the SWIPT scheme.

Chương 3: SYSTEM MODEL

In this chapter, the proposed research model comprises a base station (S) and two user devices (D1 and D2), utilizing the NOMA technique with SC mechanism at the transmitter side, and SIC mechanism at the relay station for energy harvesting. The following two cases are presented:

3.1. The first case

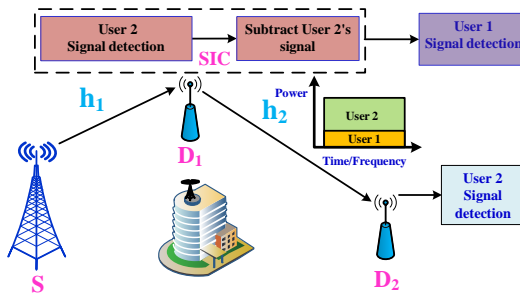


Figure 3.1: System model with one base station and two user devices with an obstruction between S and D₂.

Assuming there is an obstacle between S and D₂, as depicted in Figure 3.1, the scenario unfolds as follows: In Figure 3.1, S broadcasts two signals, namely x_1

and x_2 , to user device D_1 . Upon reception, D_1 detects the signal x_2 and regards it as interference, subsequently employing the SIC technique to eliminate x_2 from consideration. D_1 successfully decodes its own signal, x_1 , through detection. Following this, D_1 's assistance comes into play, facilitating the relay of the decoded signal x_2 from S to D_2 . This communication model involves D_1 employing the DF protocol, utilizing harvested energy received from S .

Assuming a system model with a Rayleigh fading channel, the distances from S to D_1 and from D_1 to D_2 are denoted as d_1 and d_2 , respectively. The gains within the corresponding links follow Rayleigh distributions, characterized by a probability density function (PDF) as follows:

$$f_{|h_i|^2}(x) = \frac{1}{\Omega_i} \exp\left(-\frac{x}{\Omega_i}\right), i \in \{1, 2\}, \quad (3.1)$$

where, Ω_i represents the average power and the cumulative distribution function (CDF) is determined by:

$$F_{|h_i|^2}(x) = 1 - \exp\left(-\frac{x}{\Omega_i}\right), i \in \{1, 2\}. \quad (3.2)$$

3.1.1. Energy Harvesting and Information Processing at D_1

3.1.1.1. Energy harvesting at PSR-based D_1

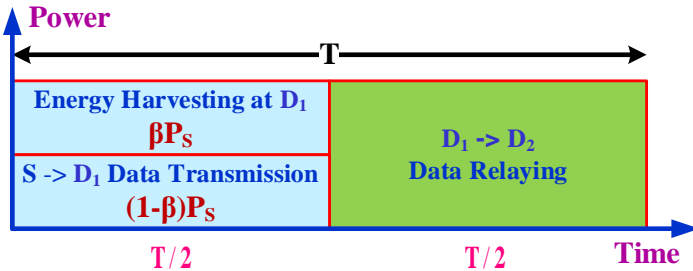


Figure 3.2: The PSR protocol of the energy harvesting system.

3.1.1.2. Energy harvesting at TSR-based D_1

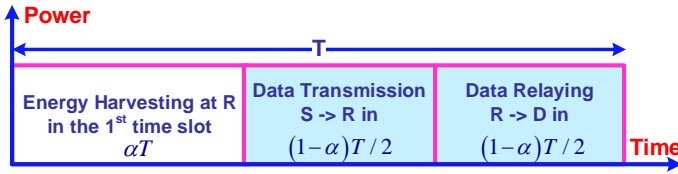
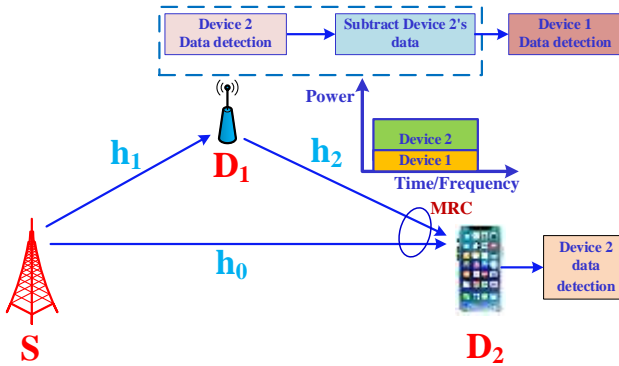


Figure 3.3: The TSR protocol of the energy harvesting system.

3.2. The second case



Hình 3.4: System model with one base station and two user devices with no obstructions between S and D₂.

Assuming an unobstructed path between S and D₂, illustrated in Figure 3.4, the scenario unfolds as follows: In Figure 3.4, two user devices, D₁ and D₂, receive the transmission signal from the base station, S. Due to the greater distance of D₂ from the source node S compared to D₁, D₁ plays a pivotal role in aiding S to relay the information to D₂.

Chapter 4: PERFORMANCE ANALYSIS

In Chapter 3, the PhD student formulated expressions for energy harvesting and information processing at the relay station for the two proposed cases. Furthermore, this chapter encompasses the development of performance formulas (including OP, throughput, ergodic rate, and EE) for the SWIPT NOMA system. The chapter proceeds to analyze and assess the system's performance under the following scenarios:

- Transmitting through the relay station and direct transmission.
- Employing perfect SIC and imperfect SIC.

4.1. Performance analysis of case 1

4.1.1. Outage probability at D₁

The outage probability at D₁ of the PSR protocol is given by:

$$P_{D_1,X} = 1 - \Pr(\gamma_{2,D_1} > \gamma_{th_2}, \gamma_{1,D_1} > \gamma_{th_1}), \quad (4.1)$$

where, $\gamma_{th_1} = 2^{2R_1} - 1$ and $\gamma_{th_2} = 2^{2R_2} - 1$ represent the threshold SNRs at D₁ for detecting signals x₁ and x₂, respectively.

$$P_{D_1,X} = 1 - e^{-\frac{\theta_{1,X}}{\Omega_1}}, \quad (4.2)$$

Set $\tau_{1,X} = \frac{\gamma_{th_2}}{\rho\psi_X'(a_2 - a_1\gamma_{th_2})}$, $\nu_{1,X} = \frac{\gamma_{th_1}}{a_1\psi_X'\rho}$ and $\theta_{1,X} = \max(\tau_{1,X}, \nu_{1,X})$ with $a_2 > a_1\gamma_{th_2}$.

4.1.2. Outage probability at D₂

$$\begin{aligned} P_{D_2,X} &= \Pr(\gamma_{2,D_1} < \gamma_{th_2}) + \Pr(\gamma_{2,D_2} < \gamma_{th_2}, \gamma_{2,D_1} > \gamma_{th_2}) \\ &= 1 - e^{-\frac{\tau_{1,X}}{\Omega_1}} + \int_{\tau_{1,X}}^{\infty} \left(1 - e^{-\frac{2\gamma_{th_2}}{x\psi_X'\rho\Omega_2}}\right) \frac{1}{\Omega_1} e^{\left(\frac{-x}{\Omega_1}\right)} dx, \end{aligned} \quad (4.4)$$

The outage probability at D₂ for high SNR is expressed by:

$$P_{D_2,X}^{\infty} = 1 - 2\sqrt{\frac{2\gamma_{th_2}}{x\psi_X'\rho\Omega_1\Omega_2}} K_1 2\sqrt{\frac{2\gamma_{th_2}}{x\psi_X'\rho\Omega_1\Omega_2}}. \quad (4.6)$$

4.1.3. Throughput for DLT Mode

$$\tau_{t,X} = (1 - P_{D_1,X})R_1 + (1 - P_{D_2,X})R_2. \quad (4.7)$$

4.1.4. Ergodic rate for DTT Mode

4.1.4.1. Ergodic rate at D₁

$$R_{D_1,X} = \frac{-e^{\left(\frac{1}{\psi_I^X a_1 \rho \Omega_1}\right)}}{2 \ln 2} Ei\left(\frac{-1}{\psi_I^X a_1 \rho \Omega_1}\right). \quad (4.9)$$

4.1.4.2. Ergodic rate at D₂

$$R_{D_2,X} = \frac{1}{2 \ln 2} \int_0^{\frac{a_2}{a_1}} \left[\frac{e^{\frac{-x}{\psi_I^X \rho (a_2 - a_1 x) \Omega_1}} + \int_0^{\infty} \frac{1}{\psi_I^X \rho (a_2 - a_1 x) \Omega_1} \left(1 - e^{\frac{-2x}{y \rho \psi_E^X \Omega_2}}\right) e^{\frac{y}{\Omega_1}} dy}{1+x} \right] dx. \quad (4.11)$$

4.1.4.3. Ergodic rate of the system

$$\tau_{r,X} = R_{D_1,X} + R_{D_2,X}. \quad (4.14)$$

4.1.5. Imperfect SIC

$$P_{x_1, D_1}^{I-SIC} = 1 - e^{-\frac{\hat{\theta}_1}{\Omega_1}}, \quad \forall \hat{\theta}_1 = \frac{\gamma_{th_1}}{\rho \psi_I (a_1 - a_2 \kappa^2 \gamma_{th_1})}. \quad (4.17)$$

4.2. Performance analysis of case 2

4.2.1. Outage probability at D₁

Similar to the outage probability at D₁ in case 1.

4.2.2. Outage probability at D₂ for the relay link

Similar to the outage probability at D₂ in case 1.

The outage probability at D₂ for high SNR is expressed by:

$$P_{D_1}^{\infty} = \frac{\theta_1}{\Omega_1}. \quad (4.18)$$

4.2.3. Outage probability at D₂ for both relay and direct link

$$\begin{aligned}
P_{D_2,dir} &= \int_0^\infty \int_0^{\psi_I \tau_I} \frac{1}{\Omega_0 \Omega_1} \left(1 - e^{-\frac{\gamma_{m2}}{x \psi_E \rho \Omega_2} + \frac{\gamma a_2}{x \psi_E \Omega_2 (y a_1 \rho + 1)}} \right) e^{-\frac{x}{\Omega_1} - \frac{y}{\Omega_0}} dx dy \\
&\times e^{-\frac{\tau_I}{\Omega_1} + \left(1 - e^{-\frac{\tau_I}{\Omega_1}} \right) \left(1 - e^{-\frac{\tau_I \psi_I}{\Omega_0}} \right)}. \tag{4.21}
\end{aligned}$$

4.2.4. Throughput for DLT Mode

4.2.4.1. User Relaying Without Direct Link

The throughput of the system over relaying without direct link is like case 1.

4.2.4.1. User Relaying with Direct Link

$$\tau_{t,dir} = \left(1 - P_{D_1} \right) R_1 + \left(1 - P_{D_2,dir} \right) R_2. \tag{4.25}$$

4.2.5. Ergodic rate for DTT Mode

4.2.5.1. Ergodic rate at D₁

The ergodic rate at D₁ over relaying without direct link is like case 1.

4.2.5.2. Ergodic Rate at D₂ for User Relaying without Direct Link

The ergodic rate at D₂ over relaying without direct link is like case 1.

4.2.5.3. Ergodic Rate at D₂ for User Relaying with Direct Link

$$R_{D_2,dir} = \frac{1}{2 \ln 2} \int_0^{\frac{a_2}{a_1}} \left[\frac{e^{-\frac{x}{\psi_I \rho (a_2 - a_1 x) \Omega_1}} - \int_0^\infty \int_x^\infty \frac{1}{\Omega_1 \Omega_0} \left(1 - e^{-\frac{2x(y a_1 \rho + 1) + 2y a_2 \rho}{z \rho \psi_E \Omega_2 (y a_1 \rho + 1)}} \right) e^{-\frac{y}{\Omega_0} - \frac{z}{\Omega_1}} dy dz}{1 + x} \right] dx \tag{4.27}$$

The ergodic rate in the asymptotic expression at D₂ for high SNR region

$$R_{D_2,dir}^\infty = \frac{1}{2 \ln 2} \int_0^{\frac{a_2}{a_1}} \int_0^\infty e^{-\frac{2x}{y\rho\Omega_2\psi_{PSR}^E} - \frac{2a_2}{a_1 y \rho \Omega_2 \psi_{PSR}^E} - \frac{y}{\Omega_1}} \frac{dx dy}{\Omega_1(1+x)}. \quad (4.29)$$

4.2.5.4. Ergodic rate of the system for User Relaying Without Direct Link

The ergodic rate of system over relaying without direct link is determined similar to case 1.

4.2.5.5. Ergodic rate of the system for User Relaying with Direct Link

$$\tau_{r,dir} = R_{D_1} + R_{D_2,dir}, \quad (4.31)$$

4.2.6. Energy efficiency

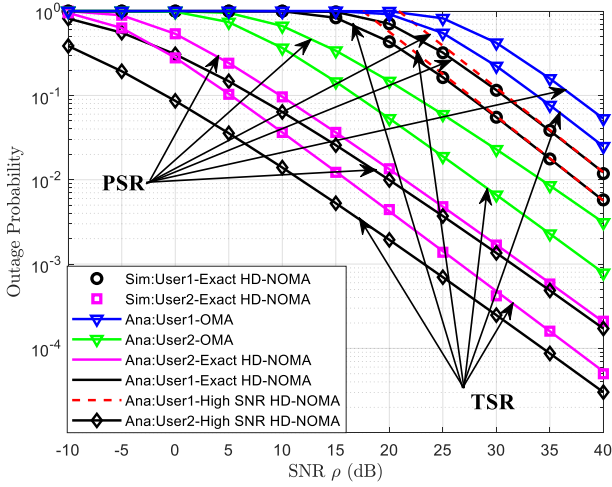
$$EE_{\phi,X} = \frac{2\tau_{\phi,X}}{TP_S + TP_r} = \frac{2\tau_{\phi,X}}{\rho(1 + \psi_E \Omega_1)}, \quad (4.32)$$

where, $T = 1$, $\sigma^2 = 1$, $\rho = \frac{P_S}{N_0}$, $P_r = \beta\eta|h_1|^2 P_S = \psi_E \Omega_1 P_S$, and $\phi \in (t, r)$, denotes the system energy efficiency in DLT mode and DTT mode, respectively.

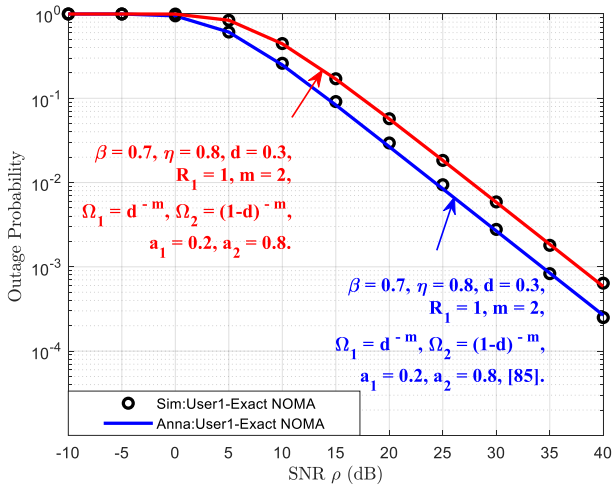
Chuong 5: RESULTS AND COMMENTS

5.1. Simulation results and comments for case 1

Figure 5.1(c)-(d) plots the OPs of two users for the PSR and TSR protocols in terms of SNR. User 2 has a lower OP than User 1 in both HD CNOMA and OMA schemes. In addition, the OP of two users in HD CNOMA scheme is lower than OP of two users in OMA scheme.

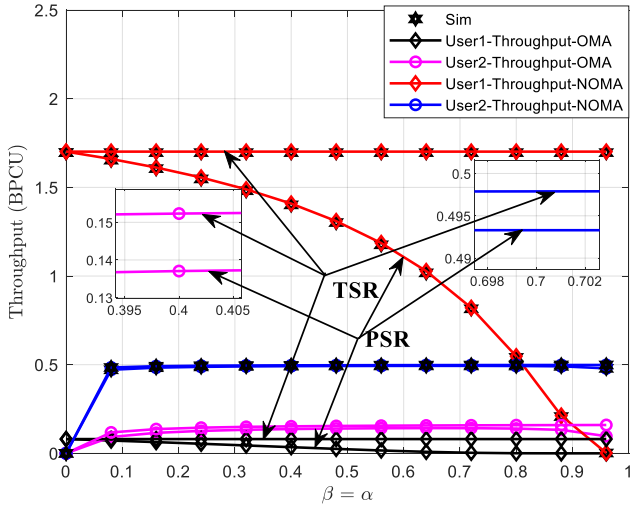


Hình 5.1c. Outage probability versus transmitting SNR for PSR and TSR protocols.



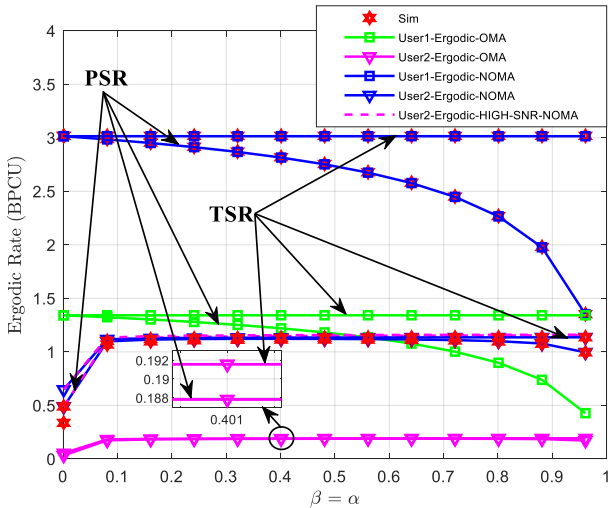
Hình 5.1d. Comparison of outage probability between this work and [85].

Figures 5.3c and 5.4c depict the throughput and ergodic rate of the two users for the PSR and TSR protocols as a function of β ($\beta=\alpha$). Specifically, we can see from Figure 5.3c that the throughput of User 1 is much higher than that of User 2 in HD CRNOMA scheme.



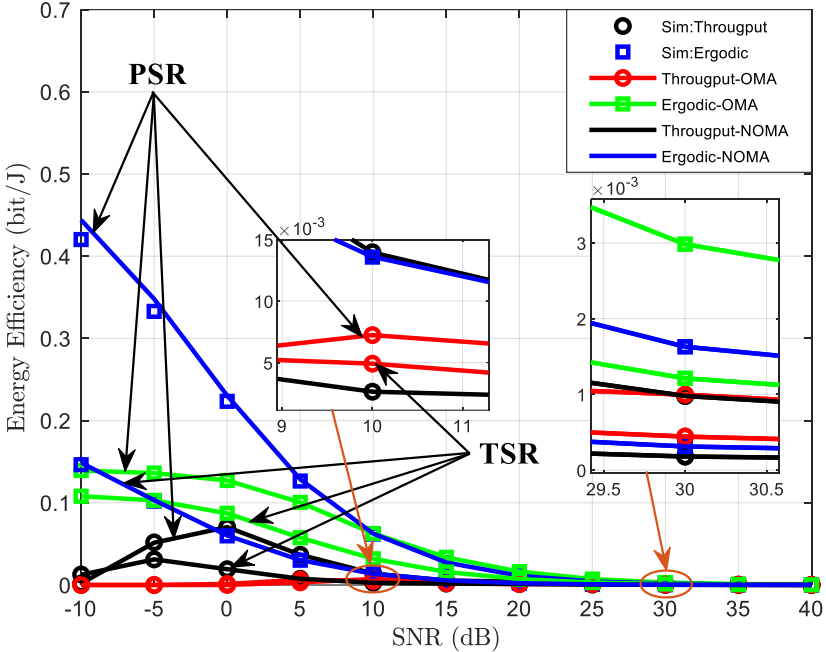
Hình 5.3c. The throughput of two users versus $\beta=\alpha$ PSR and TSR protocols.

Similarly, Figure 5.4c shows that the ergodic rate at User 1 is higher than that at User 2 in CRNOMA scheme. The ergodic rate at User 1 is the highest in the CRNOMA scheme, while the one at User 2 is the lowest in the OMA scheme.



Hình 5.4c. The ergodic rate of two users versus $\beta=\alpha$ for PSR and TSR protocols.

Hình 5.5d. plots the energy efficiency of two users for the PSR and TSR protocols as a function of SNR (dB). It can be seen that the EE performance for the DLT mode is lower than that for the DTT mode. Thus, the NOMA outperforms the EE performance as compared to the conventional OMA in low SNR region ($< 10(\text{dB})$). The reason is that the CRNOMA can achieve a larger throughput and ergodic rate than that of the OMA.



Hình 5.5d. Energy efficiency of two users for PSR and TSR protocols.

It can be observed from Fig 5.7 that the larger the distance d , the higher the outage probability of two users with NOMA.

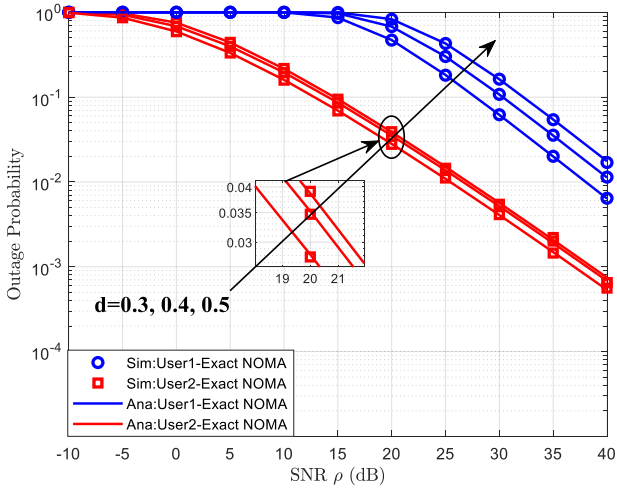
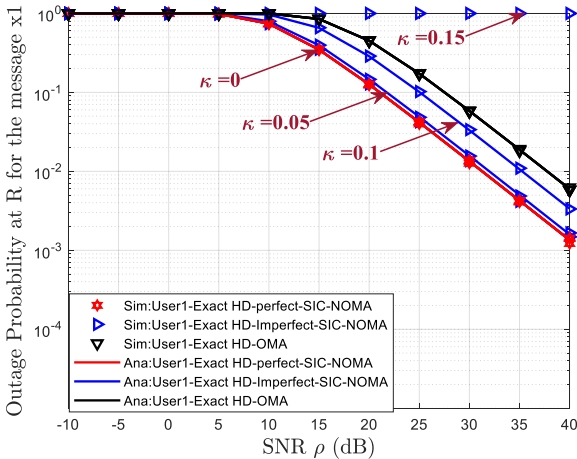
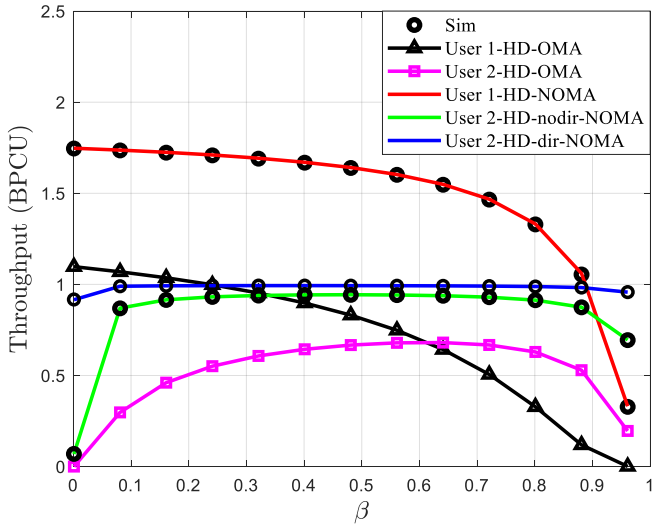


Figure 5.7. The outage probability versus SNR and different values of d .

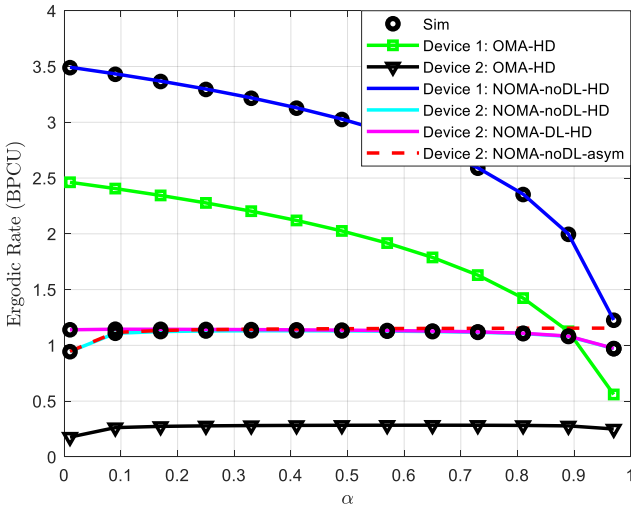
Figure 5.8 plots the comparison of the outage probabilities at D_1 versus SNR corresponding with imperfect and perfect SIC signal x_2 with different values of κ . As shown in Fig 5.8, the SIC residual interference coefficient has a considerable impact on the outage performance at D_1 .



Hình 5.8. Comparison of the outage probability at D_1 versus transmitting SNR for the cases of perfect and imperfect SIC x_2 with different values of κ .

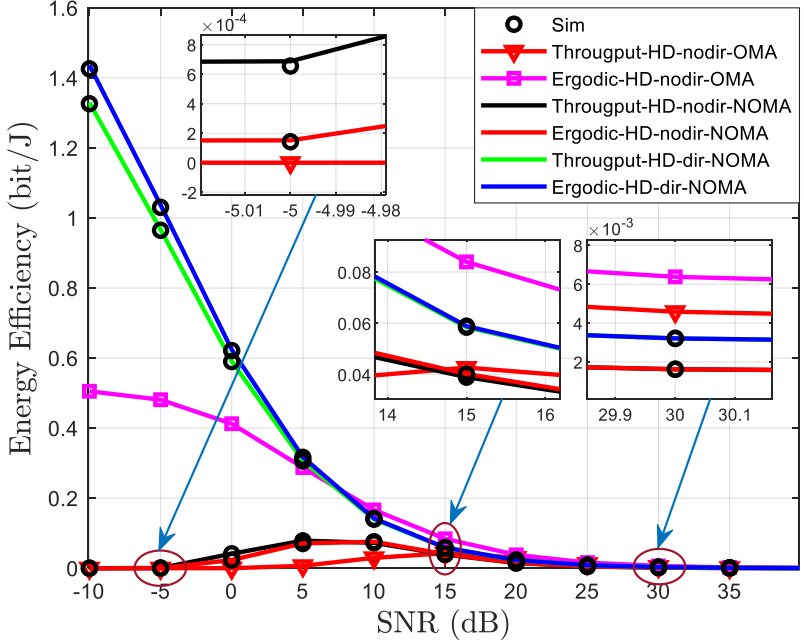


Figures 5.11. The throughput of two users versus β in cases of no direct link and direct link.



Figures 5.12. Ergodic rate of two users versus β in cases of no direct link and direct link.

Figure 5.13 illustrates the energy efficiency according to SNR from -10 to 40 dB. It is shown that the EE for C-NOMA with direct link achieves much higher than that for C-NOMA without direct link and OMA.



Hình 5.13. Energy efficiency of two users for the PSR protocol in cases of without direct link and direct link.

Chapter 6: CONCLUSIONS AND FUTURE WORKS

6.1. Conclusions

This thesis has proposed solutions to harvested energy in the SWIPT NOMA system with the focus on power domain NOMA and cooperation NOMA which has been implemented in research topics. Solutions for energy harvesting from the base station, making an important contribution to the assessment, deployment, and planning of radio networks, wireless sensor networks, and performance in environments where power cannot be provided. such as in the human body, organism, in the air or in the case of rescue, flood warning, landslide warning, forest fire warning.... Performance of research models using PSR, TSR protocols

for energy harvesting and information processing, with forward and direct pass-through methods, with DF mechanism in SWIPT NOMA system, all established by mathematical expressions, is verified through Monte-Carlo simulation results. The performance results demonstrate that NOMA outperforms OMA in both throughput and ergodic rate, PSR protocol is superior to TSR protocol.

Through this content, it is shown that the NOMA scheme is very feasible and superior to the conventional OMA scheme. From there, NOMA can be applied in a cooperative relaying network, which can be deployed in various areas of radio communication.

6.2. Future works

Continuing research on NOMA and EH contributes to overcoming challenges for relay network, wireless cooperation network is the problem of energy shortage. This thesis studies protocols to wirelessly harvest energy from RF waves in the surrounding environment and simultaneously process information in the NOMA system to extend the life of power-constrained relay stations in wireless networks developed for multi-relay, multi-antenna systems, energy harvesting cooperative relay radio access networks, wireless sensor networks, heterogeneous cloud radio access networks (H-CRAN), unmanned aerial vehicles (UAVs)...

The works that can develop from this thesis are:

- Compare and evaluate the characteristics of two PSR and TSR protocols in multi-relay, multi-access point networks; calculate the outage probability, throughput, ergodic rate, and energy efficiency of the system, for the relay and direct link; calculate the outage probability, throughput, ergodic rate and energy efficiency of the system, for both half-duplex and full-duplex transmission.
- Evaluate the performance of the H-CRAN network in energy harvesting and information processing. The main research goals are to enhance spectrum efficiency, improve energy efficiency, increase battery life for mobile devices and wireless communication systems.

LIST OF PUBLICATIONS

1. Huu Q. Tran, Phuc Q. Truong, Ca V. Phan, and Quoc-Tuan Vien, "On the energy efficiency of NOMA for wireless backhaul in multitier heterogeneous

CRAN”, In International Conference on Recent Advances in Signal Processing, Telecommunications & Computing (**SigTelCom2017**), pp. 229-234.

2. Huu Q. Tran, Ca V. Phan, and Quoc-Tuan Vien, “An overview of 5G technologies”, In Emerging Wireless Communication and Network Technologies, pp. 59-80. Springer, Singapore, (2018).

3. Huu Q. Tran, Ca V. Phan, and Quoc-Tuan Vien, “On the performance of regenerative relaying for SWIPT in NOMA Systems”, In 2019 26th International Conference on Telecommunications (ICT), pp. 1-5.

4. Huu Q. Tran, Ca V. Phan, and Quoc-Tuan Vien, (2020), “Power splitting versus time switching based cooperative relaying protocols for SWIPT in NOMA systems”, Physical Communication: 101098, (**SCIE-Q2**).

5. Huu Q. Tran, Tien-Tung Nguyen, Ca V. Phan, and Quoc-Tuan Vien, (2019), “Power-splitting relaying protocol for wireless energy harvesting and information processing in NOMA systems”, IET Communications, 13, no. 14, pp. 2132-2140, (**SCIE-Q2**).

6. Huu Q. Tran, Tien-Tung Nguyen, Ca V. Phan, and Quoc-Tuan Vien, “On the performance of NOMA in SWIPT systems with power-splitting relaying”, In 2019 19th International Symposium on Communications and Information Technologies (ISCIT), pp. 255-259.

7. Huu Q. Tran and V. T. Nguyen (2020), "Biometric Image Recognition For Secure Authentication Based on FPGA: A survey", 5th International Conference on Green Technology and Sustainable Development (GTSD), pp. 618-623, doi: 10.1109/GTSD50082.2020.9303115.

8. Huu Q. Tran, Ca V. Phan, and Quoc-Tuan Vien, (2021), "Performance analysis of power-splitting relaying protocol in SWIPT based cooperative NOMA systems," EURASIP Journal on Wireless Communications and Networking, pp.110-136, <https://doi.org/10.1186/s13638-021-01981-9>, (**SCIE-Q2**).

9. Huu Q. Tran, Ca V. Phan, and Quoc-Tuan Vien, (2021), "Optimizing Energy Efficiency for Supporting Near-Cloud Access Region of UAV-Based NOMA Networks in IoT Systems", Wireless Communications and Mobile Computing, vol. 2021, Article ID 4345622, 12 pages, <https://doi.org/10.1155/2021/4345622>, (**SCOPUS-Q2**).